Journal on Surgery

www.journalonsurgery.org

Research Article

Open Access, Volume 3

Technical Features of the Experimental Target Device for Denervation of the Pulmonary Arteries

Trofimov NA; Egorov DV*; Nikolskiy AV; Rodionov AL; Ivanov DS

Chuvash State University, 15 Moskovskiy Prospekt, 428015 Cheboksary, Russia.

Abstract

Objectives: Creation of a device that allows additionally performing a procedure to correct high pulmonary hypertension during heart valve replacement surgery.

Methods: In laboratory conditions, a number of parameters of the pulmonary vessels were measured - the wall thickness in various areas, the diameter of the pulmonary trunk in the initial state (without squeezing it) and the transverse size of the pulmonary trunk when squeezing until its inner walls were completely closed.

Results: The main power and geometrical parameters that should be provided for the developed experimental sample of an electrosurgical instrument during radiofrequency ablation of the pulmonary artery trunk with the aim of its denervation are determined.

Conclusion: The created device-ablator will allow the most effective and safe impact on the wall of the pulmonary artery in order to correct pulmonary hypertension.

Keywords: Secondary pulmonary hypertension; Pulmonary arteries denervation; Mitral valve disease; Atrial fibrillation.

Abbreviations: PA: pulmonary arteries; PH: pulmonary hypertension.

Introduction

Pulmonary Hypertension (PH) almost always occurs with long-term rheumatic and degenerative heart disease. Performing surgery only on the affected heart valve with pre-existing PH often does not lead to normalization of blood pressure in the Pulmonary Artery (PA) [1-3]. To improve the long-term results of surgical correction in the last few years, it is recommended to perform denervation of the trunk and orifices of the PA simultaneously with surgical correction of the affected heart valves [4-6]. The applied thermal effect damages the sympathetic plexuses, which leads to a complete or partial removal of the tonic effect of the sympathetic nervous system on the capillary bed in the lung tissue. This causes the removal of vascular spasm and reduces pressure in the PA itself and its branches. Currently used devices for denervation of the PA are developed in cardiac surgery only for ablation of arrhythmogenic zones of the atria of the myocardium itself. Specialized devices for radiofrequency ablation of the walls of the PA have not yet been developed. We propose the creation of a spe-

Manuscript Information: *Received: Mar 07, 2023; Accepted: Mar 30, 2023; Published: Apr 06, 2023*

Correspondance: *Egorov Dmitrii Vladimirovich, Chuvash State University, 15 Moskovskiy Prospekt, 428015 Cheboksary, Russia.*

Email: meddevil@mail.ru

Citation: *Trofimov NA, Egorov DV, Nikolskiy AV, Rodionov AL, Ivanov DS. Technical Features of the Experimental Target Device for Denervation of the Pulmonary Arteries. J Surgery. 2023; 3(1): 1086.*

cialized bipolar ablator for effective impact on the vascular wall of the PA.

Materials and methods

According to the results of the search for analogues and products that solve similar problems, carried out among patent documentation, literary sources, advertising materials, company websites, we were unable to identify devices that would be used in open heart surgery to correct PH by acting on the outer wall bifurcation region of the PA for the purpose of its denervation.

In our clinical practice, since 2016, we have been using a modified method [4,6] to perform circular denervation of the trunk and orifices of the PA using an AtriCure® Isolator® Synergy™ Clamps device for the treatment of atrial fibrillation (USA) together with Ablation Sensing Unit RF generator (USA) (Figure 1) [7,8].

The device-ablator created by us was also made in the form of a clamp with parallel-joining jaws having a constant geometry and a gap between the jaws of no more than 40 mm, with an electrode system located on them. The clamping structure of the device, as well as its close analogue, is designed for stable fixation of the position and uniform compression of the vessel tissues until the walls of the PA are in full contact with each other. At the same time, the following zones of the PA vascular wall located between the branches of the ablator clamp can be clearly distinguished: the anterior and posterior walls of the PA, as well as the places of folds, which we designated as the "marginal zones" of the wall of the occluded vessel (Figure 2) [9].

One of the most important parameters of the final device, which ensures optimal PA denervation, is the force with which the ablator electrodes compress the PA walls. To calculate the optimal compression force of the jaws of the ablator clamp, the bifurcation complex of the PA trunk was taken from deceased people aged 54 to 66 years, with relatively unchanged walls of the trunk and main branches of the PA. The research work was approved by the local ethics committee.

In laboratory conditions, a number of parameters of the pulmonary vessels were measured - the wall thickness in various areas, the diameter of the pulmonary trunk in the initial state (without squeezing it) and the transverse size of the pulmonary trunk when squeezing until its inner walls were completely closed.

The internal diameter of the pulmonary trunk in the initial state was measured using smooth plug gauges with inserts with a diameter of 20 mm to 40 mm (GOST 14810-69) with a measurement step of 1 mm. The inner diameter of the pulmonary trunks was 25…32 mm.

The wall thickness of the pulmonary trunks was measured using a digital caliper Matrix 31611 - 150 mm - 0.01 with a division value of 0.01 mm and a measurement error of 10 µm. After these measurements, it was found that the circumferential thickness of the artery wall is almost always the same (h1 ~ h2 ~ h3 ~ h4) and its average value is 1.2 ± 0.05 mm (Figure 3).

Results

The measurement data made it possible to calculate the depth of circular thermal damage to the PA wall, which is necessary for its optimal desympathization, based on the histological data on the structure of the wall of this vessel. It is known that the wall of the PA consists of three layers of different thickness (Figure 4). At the same time, sympathetic fibers are located in the adventitial (superficial) layer of the PA wall, immersing as much as possible only to the middle third of the middle layer (media) [10-13]. Thus, based on the average thickness of the layers of the PA wall, known from the literature, it can be calculated that for complete sympathization of the pulmonary trunk, irreversible damage to the wall of this vessel is necessary to a depth of no more than 0.7 mm, which is 58% of the thickness of the vessel wall. On the basis, two zones of damage to the PA wall were identified, which occur with optimal RF exposure (Figure 4):

Zone I - zone of irreversible thermal damage to the wall of the PA;

Zone II - the zone of viability of the PA wall.

The division of the PA wall into two zones under RF exposure makes it possible to carry out irreversible damage to all sympathetic trunks in zone I, thereby causing persistent and effective desympathization of the pulmonary vascular bed, and in zone II, due to the preservation of baroreceptors in the intimal (inner layer) of the vessel, to give the opportunity to continue to carry out the regulation of the reflex reaction of the vessels of the pulmonary circulation through the baroreceptors. The latter are localized in the intimal layer of the pulmonary trunk and the main branches of the PA. With an increase in pressure in the PA, the indicated baroreceptors are excited, located mainly in the area of the bifurcation of the pulmonary trunk, which in turn reflexively reduces pressure in the systemic circulation by slowing down the heart and dilating the vessels of the systemic circulation. This leads to the deposition of blood in the body and a decrease in its flow to the lungs (the so-called Parin reflex). The physiological significance of this reflex is that, by unloading the pulmonary circulation, it prevents the development of pulmonary edema and decompensation of the pulmonary circulation [14-16].

It should also be taken into account that when squeezing between the jaws of the clamp-ablator of the pulmonary vessel, a complex deformed state occurs in its wall, characterized in different places of the vessel wall by a different ratio of compressive and tensile stresses and deformations. In particular, in case of contact of the inner wall of the vessel along its entire perimeter, the thickness of the artery wall will decrease due to the deformation of its compression (Figure 5).

The degree of deformation of the vessel wall can be expressed through the relative compression strain of the vessel wall ε, which is determined by the formula:

$$\varepsilon = [(h_o - h) / h_o] \cdot 100\% \ [\%], \quad (1)$$

where ho, h are the thickness of the PA wall in the initial state and after its compression.

A series of experiments was carried out to determine the pressure p that must be applied when squeezing the pulmonary trunks in order to achieve a state where the inner wall of the artery would be in contact along its entire perimeter. Such a state was usually referred to as the "final state" (Figure 5).

In order to determine this pressure and the relative degree of deformation of the artery wall corresponding to it, on a stand specially created for this purpose (Figure 6), the trunk of the PA was placed on the base 1, after which the movable traverse 2 was installed on the guide pins 3, and in this state the stand with the PA placed there the barrel was installed in a portable lever press (Figure 7).

In order to compress the PA placed in the stand, a force P was applied to its movable traverse, which was created due to the fact that a load G, fixed by an electronic steelyard, was applied to the end of the press lever. For a more accurate task of the load G, sets of analytical weights were used with a selection accuracy of up to 1 gram.

Applying a load G to the end of the lever of the press ensured, due to it and the stand pivotally connected to it, resting with the other end on the movable traverse of the stand, the creation of a load P on the artery trunk. The loading was carried out until the "final state" arrived, i.e. complete closure (contact) of the inner wall of the vessel along its entire perimeter. In this case, the assessment of the complete contact of the wall was recorded using a single-beam electron-optical system, the essence of which is that the light beam emerging from the LG-75 laser, passing through the ZRT-457 telescope, enters the attachment, the optical slit of which cuts out from this wide beam - a narrow beam of rectangular cross section, which then passes through a polarizing light filter and is directed to a longitudinally compressed arterial trunk. At the moment when there is any lumen in the compressed artery, the beam hits the cathode of the FEU-83 photomultiplier (with power supply unit VS-22) connected by a shielded cable to the S8-2 storage oscilloscope. The signal on the oscilloscope is directly proportional to the amount of light flux that hit the cathode of the photomultiplier tube, which in the same way depends on the transverse area of the beam. At the moment of complete closure of the inner wall of the vessel, the transverse area of the beam becomes equal to zero, and this is displayed on the oscilloscope screen by the absence of a signal (the curve goes into a horizontal zero line). At this moment, the force G applied to the press lever was recorded, which was recalculated as the force P applied to the movable traverse of the stand, as well as the vertical movement of the movable traverse, fixed by the dial indicator CHIZ 45735 (accuracy class 1, measurement range - 0 ... 10 mm , measurement step - 0.01 mm, measurement error - 20 µm) shown in **Figure 5**. This movement was used to evaluate the decrease in the thickness (two thicknesses) of the pulmonary trunk wall under dosed pressure applied to it until the vessel was completely closed. In this "final state", the width of the compressed vessel was also measured using a digital caliper Matrix 31611 - 150 mm - 0.01 with a division value of 0.01 mm and a measurement error of 10 µm.

All the data obtained were recorded in a table and, on their basis, the corresponding calculations were made. In particular, the pressure p was calculated, which occurred when the inner wall of the vessel was completely closed under the action of force P on the upper and lower areas of contact of the squeezed vessel, respectively, with the movable traverse or stand base:

$$p = P / F = P / (a \cdot b) \text{ [N/mm2 = MPa]}, \quad (2)$$

where F – the contact area of the squeezed vessel with the movable traverse (or base) of the stand, mm2;

a – the contact width of the squeezed vessel with the movable traverse (or base) of the bench, mm;

b – he length of the contact of the vessel in its longitudinal direction with the movable traverse (or base) of the stand, mm.

In particular, the measurements showed that the parameter a ranged from 36.2 mm to 45.1 mm, and the parameter b in the calculations was taken, in accordance with Figure 4, equal to 6 mm.

Calculations have shown that the "final state" of the squeezed vessel occurs at pressure p, the average value of which is 0.045 MPa. At the same time, it turned out that the wall thickness of the pulmonary trunk h decreased to an average of 1.02 mm and the relative deformation of its compression ε averaged 15%.

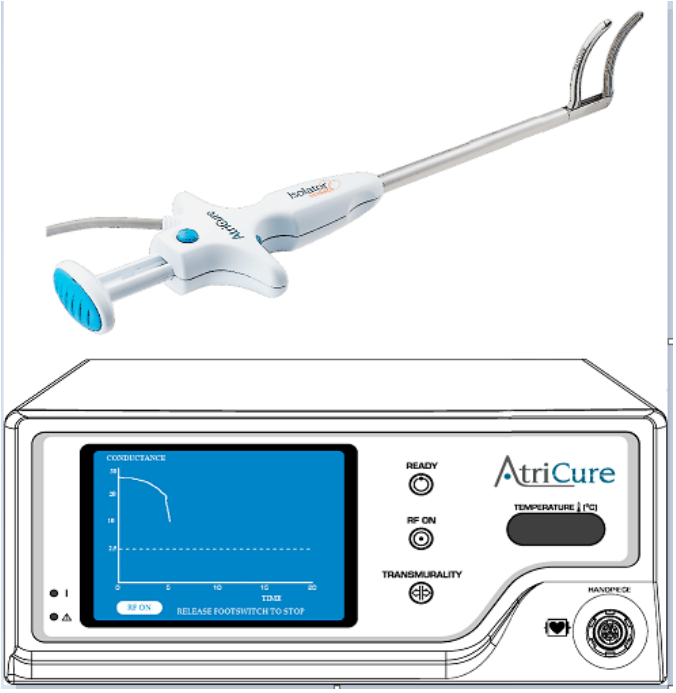

Figure 1: AtriCure® Isolator® Synergy™ Clamps and Ablation Sensing Unit RF generator (USA).

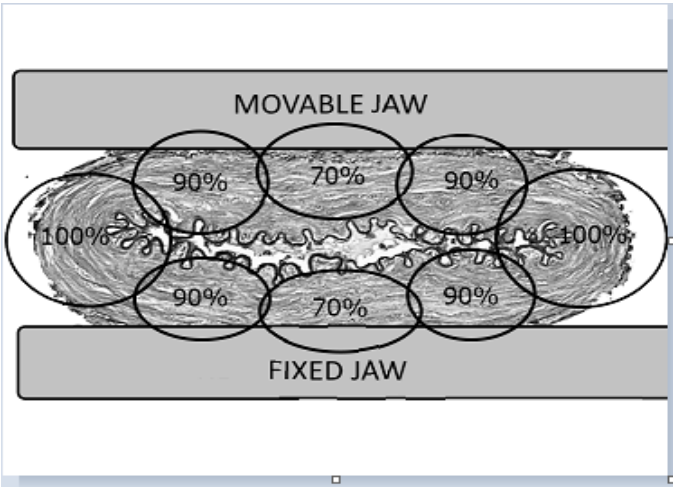

Figure 2: Compression of PA walls and formation of "marginal zones".

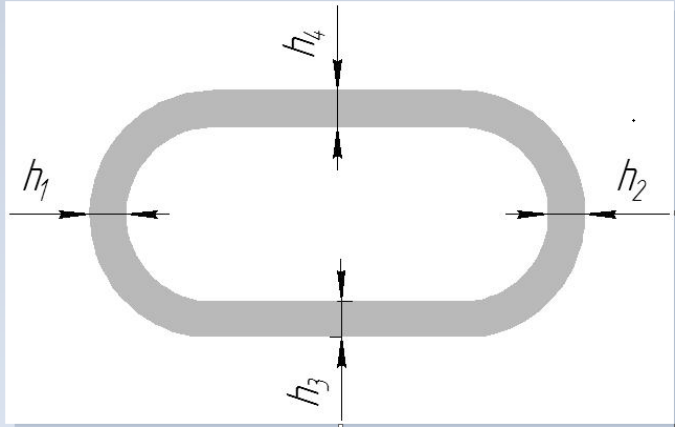

Figure 3: Scheme for measuring the thickness of the PA wall.

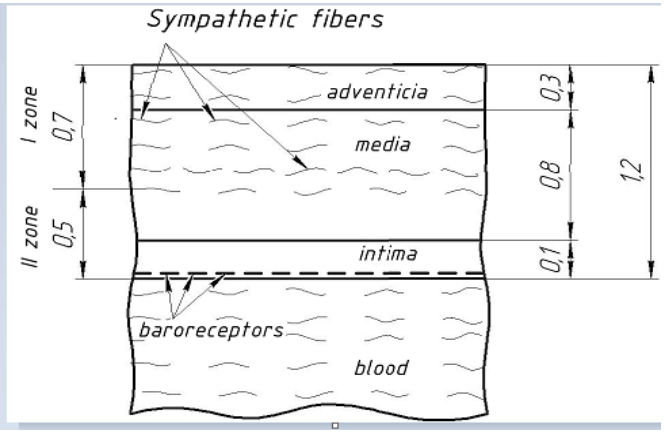

Figure 4: Schematic drawing of the structure of the PA wall.

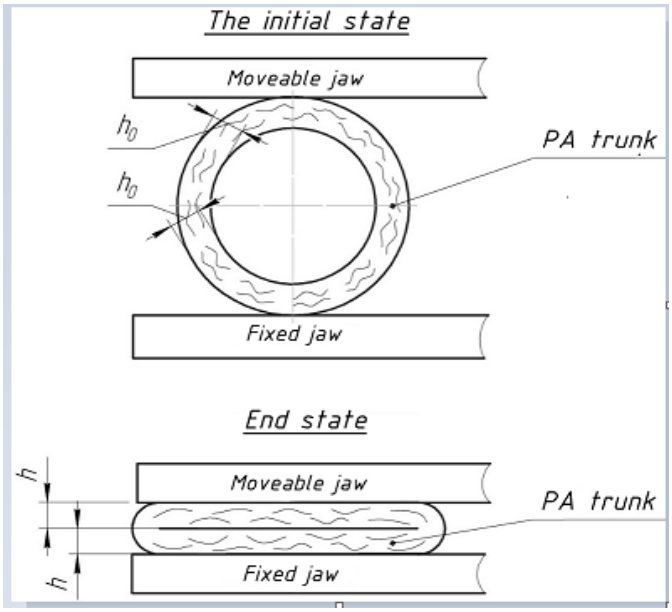

Figure 5: Schematic representation of PA deformation when it is squeezed between the jaws of the ablator clamp.

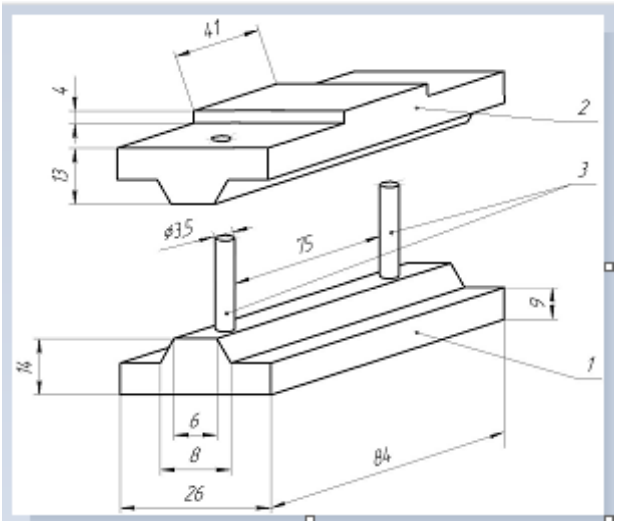

Figure 6: Stand for transverse compression of the trunk of the PA: 1 - base; 2 - movable traverse; 3 - guide pins.

Figure 7: Portable lever press with a stand mounted on it for transverse compression of the PA trunk.

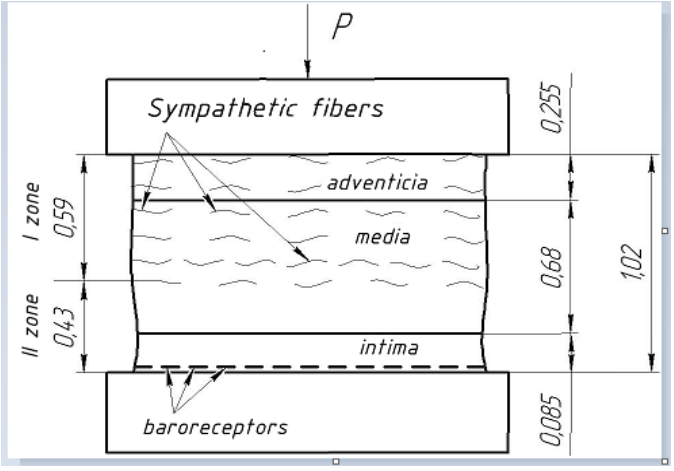

Figure 8: Estimated thicknesses of the pulmonary trunk wall layers when it is compressed by 15% and the depth of the optimal RF exposure to the compressed vessel wall.

Discussion

Thus, on the basis of the conducted experimental studies with "fresh" pulmonary trunks, it was established that in order to compress the pulmonary artery trunk on the above stand until the inner surface of the artery wall is completely closed, it is necessary to apply a force P transverse to the vessel, the value of which will depend not only on the value of the given above the average value of pressure p, but also on the contact area of the squeezed vessel with the movable traverse (or base) of the stand F=a•b. In the experiments performed, this force was in the range from 0.89 kg (~8.08 N) to 1.21 kg (~11.12 N).

Based on the foregoing, the thicknesses of the pulmonary trunk wall layers were calculated, which will occur when this vessel is compressed until the surface of its inner wall is completely closed (Figure 8), i.e. with a decrease in its thickness by 15%, assuming that the thickness of each layer of the compressed vessel wall will also decrease by 15%.

Taking into account the decrease in the thickness of the layers of the wall of the pulmonary trunk with the application of the optimal calculated compression pressure until the vessel is completely closed and the previously indicated zone of damage with optimal RF exposure to the wall of the pulmonary trunk with a depth of 58% of its thickness, the depth of such a zone was also determined during RF exposure to the compressed vessel. It was 0.59 mm (Figure 8).

Thus, as a result of the experimental work, the main power and geometric parameters were determined, which should be provided for the developed experimental model of an electrosurgical instrument during radiofrequency ablation of the pulmonary artery trunk in order to denervate it [17].

Declarations

Conflict of interest: None declared.

Funding: This work is supported by the Russian Science Foundation under grant 21-75-10075.

References

1. Guazzi M, Vitelli A, Labate V, Arena R. Treatment for pulmonary hypertension of left heart disease. Current treatment options in cardiovascular medicine. 2012; 14: 319-327.
2. Briongos Figuero S, Moya Mur JI, Garcia-Lledo A, Centella T, Salido L, et al. Predictors of persistent pulmonary hypertension after mitral valve replacement. Heart and vessels. 2016; 31: 1091-1099.
3. BABOKIN V, TROFIMOV N. Prevention of Atrial Fibrillation Recurrence After the Maze IV Procedure. The Annals of Thoracic Surgery. 2020; 109: 1624-1625.
4. Trofimov NA, Medvedev AP, Babokin VE. Effect of circular sympathetic denervation of pulmonary arteries on the degree of pulmonary hypertension in patients with mitral valve pathology and atrial fibrillation. Journal of clinical and experimental surgery. 2009; 4: 32-41.
5. Chen SI, Zhang FF, Xu J, Xie DJ, Zhou L, et al. Pulmonary artery denervation to treat pulmonary arterial hypertension: the single-center, prospective, first-in-man PADN-1 study (first-in-man pulmonary artery denervation for treatment of pulmonary artery hypertension). Journal of the American college of cardiology. 2013; 62: 1092-100.
6. TROFIMOV NA, MEDVEDEV AP, NIKOLSKY AV, KICHIGIN VA, ZHAMLIKHANOVA SS, et al. Denervation of Pulmonary Arteries in Patients with Mitral Valve Defects Complicated by Atrial Fibrillation and Pulmonary Hypertension. Sovremennye tehnologii v medicine. 2019; 11: 95-105.
7. HAENSIG M, RASTAN AJ, HOLZHEY DM, MOHR FW, GARBADE J. Surgical therapy of atrial fibrillation. Cardiol Res Pract. 2012; 149503.
8. MELBY SJ, SCHUESSLER RB, DAMIANO RJ. Ablation technology for the surgical treatment of atrial fibrillation. ASAIO J. 2013; 59: 461-468.
9. TROFIMOV NA, NIKOLSKIY AV, RODIONOV AL, EGOROV DV. Histological Study of Pulmonary Artery Denervation. Opera medica et physiologica. 2021; 8: 74-82.
10. KAWASHIMA T. The autonomic nervous system of the human heart with special reference to its origin, course, and peripheral distribution. Anat Embryol (Berl). 2005; 209: 425-438.
11. SCHOTTEN U, VERHEULE S, KIRCHHOF P, GOETTE A. Pathophysiological mechanisms of atrial fibrillation: a translational appraisal. Physiol Rev. 2011; 91: 265-325.
12. KIMURA K, IEDA M, FUKUDA K. Development, maturation, and transdifferentiation of cardiac sympathetic nerves. Circ Res. 2012; 110: 325-336.
13. SEKI A, GREEN HR, LEE TD, HONG L, TAN J, et al. Sympathetic nerve fibers in human cervical and thoracic vagus nerves. Heart Rhythm. 2014; 11: 1411-1417.
14. BAYLEN BG, EMMANOUILIDES GC, JURATSCH CE, YOSHIDA Y, FRENCH WJ, CRILEY JM. Main pulmonary artery distention: a potential mechanism for acute pulmonary hypertension in the human newborn infant. The journal of pediatrics. 1980; 96: 540-544.
15. JURATSCH CE, JENGO JA, CASTAGNA J, LAKS MM. Experimental pulmonary hypertension produced by surgical and chemical denervation of the pulmonary vasculature. Chest. 1980; 77: 525-530.
16. OSORIO J, RUSSEK M. Reflex changes on the pulmonary and systemic pressures elicited by stimulation of baroreceptors in the pulmonary artery. Circulation research. 1962; 10: 664-667.
17. EGOROV DV, TROFIMOV NA, DRAGUNOV AG, SHALUNOV EP. Device for radio-frequency ablation of pulmonary vessels. Patent RF RU2763939C1. 2021.